



One-pot extraction of nanocellulose from raw durian husk fiber using carboxylic acid-based deep eutectic solvent with *in situ* ultrasound assistance

Jocelyn Jean Yi Lim^a, Do Yee Hoo^a, Siah Ying Tang^b, Sivakumar Manickam^c, Lih Jiun Yu^d, Khang Wei Tan^{a,*}

^a School of Energy and Chemical Engineering, Xiamen University Malaysia, 43900 Sepang, Selangor Darul Ehsan, Malaysia

^b Chemical Engineering Discipline, School of Engineering, Monash University Malaysia, 47500 Bandar Sunway, Selangor Darul Ehsan, Malaysia

^c Petroleum and Chemical Engineering Department, Faculty of Engineering, Universiti Teknologi Brunei, BE1410, Bandar Seri Begawan, Brunei Darussalam

^d Faculty of Engineering, Technology, and Built Environment, UCSI University Kuala Lumpur Campus, No. 1, Jalan Menara Gading, UCSI Heights (Taman Connaught), Cheras 56000 Kuala Lumpur, Malaysia

ARTICLE INFO

Keywords:

Ultrasound
Extraction
Nanocellulose
One-pot reaction
Deep eutectic solvent

ABSTRACT

Nanocellulose (CNF) has emerged as a promising alternative to synthetic petroleum-based polymers, but the conventional preparation process involves multiple tedious steps, heavily dependent on chemical input, and proves cost-inefficient. This study presented an, *in situ* ultrasound-assisted extraction using deep eutectic solvent (DES) based on choline chloride and oxalic acid for more facile production of CNF from raw durian husk fibers. FESEM analysis confirmed the successful extraction of web-like nanofibril structure with width size ranging from 18 to 26 nm. Chemical composition analysis and FTIR revealed the selective removal of lignin and hemicellulose from the raw fiber. As compared to post-ultrasound treatment, *in situ* ultrasound-assisted extraction consistently outperforms, yielding a higher CNF yield with finer fiber width and significantly reduced lignin content. Integrating this eco-friendly *in situ* ultrasonication-assisted one-pot extraction method with a 7.5 min interval yielded the highest CNF yield of 58.22 % with minimal lignin content. The superior delignification ability achieved through the proposed *in situ* ultrasound-assisted protocol surpasses the individual efficacy of DES and ultrasonication processes, neither of which yielded CNF in our experimental setup. This single-step fabrication process significantly reduces chemical usage and streamlines the production steps yielding web-structured CNF that is ideal for sustainable application in membrane and separator.

1. Introduction

The substantial increase in the global population, rapid urbanization, and increased anthropogenic activities contribute significantly to the extensive generation of agricultural waste. Without proper waste management, the long-term accumulation of this agricultural waste poses a severe threat to the environment and human health. Hence, it is imperative to formulate effective waste management strategies to address environmental concerns and promote a circular economy. Over the past few decades, there has been a growing interest in upcycling lignocellulosic biomass into high-value products, such as valuable green chemicals, sought-after biofuels, and carbonaceous materials, as a means of biomass valorization [1]. Given the nutritional value and

popularity of durians in the food processing industry, durian waste has emerged as a notable agricultural waste stream with substantial potential in Southeast Asia [2]. Notably, durian husk fibers are rich in fiber content, making them exceptionally suitable for valorisation into valuable products [3].

Nanocellulose (CNF), defined as nano-scaled cellulose fragments with inherently desirable commercial properties, has become a focal point in biomass upcycling research. Its lightweight, nanoscale crystalline and fibril structure, and exceptional mechanical and optical properties position CNF as an extraordinarily versatile and sustainable material with applications spanning various sectors. When used independently, CNF exhibits remarkable emulsifying properties [4]. Moreover, when employed as a reinforcing agent in combination with

* Corresponding author.

E-mail address: khangwei.tan@xmu.edu.my (K.W. Tan).

<https://doi.org/10.1016/j.ultsonch.2024.106898>

Received 16 March 2024; Received in revised form 27 April 2024; Accepted 5 May 2024

Available online 7 May 2024

1350-4177/© 2024 Published by Elsevier B.V. This is an open access article under the CC BY-NC-ND license (<http://creativecommons.org/licenses/by-nc-nd/4.0/>).

different materials, CNF demonstrates outstanding capabilities, expanding its potential applications to diverse areas such as water remediation [5], food packaging [6], energy conversion and storage [7], biomedical applications, etc [8]. Consequently, the utilization of CNF has the potential to reduce global dependence on petroleum-based products significantly and decelerate the depletion rate of fossil fuels [9]. However, concerns have arisen about the sustainability and high cost of CNF extraction methods due to their tedious, energy-intensive, and hazardous chemical nature [10]. To address these issues and facilitate industrialization, there is a need for robust technologies that streamline the production process, from pretreatment to the extraction of surface-modified CNF, improving overall production efficiency and sustainability.

Recognizing their appealing physicochemical properties, including negligible vapor pressure and high recyclability, deep eutectic solvents (DESs) emerge as promising environmentally friendly and low-toxic solvents capable of fractionating various biopolymers through multifaceted mechanisms. Comprising hydrogen bond donor (HBD) and acceptor (HBA) components, DES can selectively cleave ester, ether, and glycosidic linkages connecting lignin and hemicellulose via proton-attacked hydrolysis. Additionally, they disrupt the overall hydrogen-bond network within interchains through an electron-withdrawing effect [11]. Extensive research has demonstrated the efficacy of carboxylic acid-based DES, such as choline chloride (ChCl)/lactic acid (LA), in delivering simultaneous delignification and hemicellulose removal at high efficiency, reaching up to 91 % [12]. This simultaneous action is unattainable by conventional methods relying solely on protons for structure deconstruction. The same category of DES has recently been explored for its performance in CNF extraction [13]. High yields of CNF were successfully extracted from various biomass feedstocks using ChCl/oxalic acid (OA) DES under conditions of 70–150 °C and 0.5–6 h, with assistance from post-mechanical treatments such as high-pressure homogenization [14], ball milling, etc [15,16]. DES effectively depolymerizes the amorphous domains of cellulose, as indicated by a decreased degree of polymerization value after treatment. Furthermore, the as-obtained CNF was found to be surface-functionalized with carboxyl groups provided by DES [17]. While previous studies have demonstrated the profound ability of DES in separate processes of pretreatment and isolation for CNF preparation, it is worth exploring the feasibility of a one-pot extraction of cnf directly from raw fibers using ChCl/OA.

In CNF extraction within a DES system, elevated temperatures contribute to a higher degree of particle size reduction due to an increased hydrolysis rate. At the same time, extended durations result in an increased degree of carboxylation [18]. However, achieving desirable CNF properties through such kinetics increases energy requirement. Ling et al. introduced microwave assistance into the DES-based pretreatment process to address this issue, resulting in rapid and intensified delignification. This enhancement facilitates cellulose extraction with high crystallinity, which can be further converted into CNF efficiency [19]. The microwave-assisted DES system expedites selective bond cleavage during lignin depolymerization. It drastically reduces processing time to just 10 min, unlike the conventional synthesis process, which requires at least 6 h of heating [20]. The use of external supplementary energy in this manner proves effective in decoupling productivity from energy demand. Moreover, ultrasonication offers an additional advantage over microwave irradiation. Its intrinsic cavitation effects disrupt solid surfaces and subsequent mass transfer into inter- and intra-fiber pores [21]. The implementation of ultrasound-assisted extraction perturbs the biomass matrices, and the cavitation bubbles produced facilitate the disruption of hydrogen bonds and penetration of the solvent into the entangled biomass network [22,23]. Specifically, these cavitation bubbles create localized shear forces, and turbulence which can highly bolster the mass and heat transfer within the reaction system. As a result, the surface of the biomass can be effectively disrupted, revealing fresh solid surfaces for delignification and cellulose

isolation. This disruption reduces diffusion boundary layers, enabling the solvent to penetrate the previously unreachable internal solid matrix, thereby enhancing the efficacy of chemical treatments [24]. Guo et al. integrated *in situ* ultrasonication (315 W, 45 °C) into nanocellulose extraction using sulphuric acid hydrolysis and achieved an improved yield of nanocellulose (18.3 % to 52.8 %) with a reduced processing time (120 min to 45 min) [25]. This suggests incorporating ultrasound-assisted extraction (UAE) improves CNF extraction efficiency under milder conditions than conventional extraction methods. Besides, the sequence of ultrasonication implementation and the duration of ultrasound irradiation can significantly influence the delignification ratio and CNF extraction yield. Specifically, ultrasound irradiation intervals can control the solvent's viscosity and the mass transfer within the solvent system, potentially affect lignin removal efficiency and CNF production yield [26,27]. Therein, this study investigated the impact of post and *in situ* ultrasonication-assisted treatments on the properties of CNF.

Considering the favourable mechanistic behaviours and environmentally benign nature of both DES and ultrasonication technology, their combined deployment offers a promising green solution for CNF extraction, aligning with green chemistry and economic chemistry principles. Therefore, this study explores the potential of using a greener and more sustainable ultrasonication-assisted DES treatment in a one-pot approach for preparing CNF from durian husk fiber. A comparison between a sequential DES-ultrasonication method and an *in situ* ultrasound-assisted protocol is conducted to elucidate the extent of performance improvement. Furthermore, the effects of the time interval between each *in situ* sonication cycle are also unraveled in this work.

2. Material and methods

2.1. Materials and reagents

The durian husk fibers were purchased from local fruit stall and ground into fine fiber (0.5 mesh) using a grinding machine after oven-drying at 60 °C. Oxalic acid dihydride (OA; R&M), and choline chloride (98 % C₅H₁₄NClO, ChCl; Chemiz) was used for the preparation of DES.

2.2. Preparation of DES

The binary DESs were prepared following the method outlined by Hong et al [28]. In brief, ChCl and OA were mixed in a molar ratio of 1:1 under constant magnetic stirring at 100 °C in an oil bath for 20 min.

2.3. Production of CNF

2.3.1. Post-ultrasonication treatment

Durian husk fiber was added into the as-prepared DES at a fiber-to-solvent weight ratio of 1:20 and stirred under 80 °C for 1.5 h. Following this, twice the volume of cold deionized water (42 mL) was added to the mixture to halt the reaction promptly. The mixture was then centrifuged at 6000 rpm for 10 min to separate DES as supernatants for recycling purpose. The sediments containing DES-treated fibers were subjected to dialysis using a dialysis membrane (12,000–14,000 Da) against water until a constant pH was attained. Subsequently, the DES-treated fibers were diluted to 0.5 wt% in deionized water and subjected to high-intensity ultrasonication (TU-1800E4, Toption Instruments, China, horn-type ultrasound reactor, 50 kHz, 1800 W, 2/2 s on/off pulse) at 900 W for 15 min to yield CNF. As not all samples were characterized in solid form, the resulting CNF suspension was not immediately isolated from the solution following ultrasonication. The obtained CNF suspension was alternatively stored in a refrigerator prior to characterization.

2.3.2. *In situ* ultrasonication-assisted treatment

Durian husk fiber was added into the as-prepared DES at a fiber-to-solvent weight ratio of 1:20 and stirred under 80 °C. Throughout the reaction at various time intervals (5, 7.5, 10 min), the mixture was subjected to high-intensity ultrasonication at 900 W for 1 min. This duty cycle was repeated for 1.5 h. Subsequently, twice the volume of cold deionized water (42 mL) was added to the mixture to halt the dissolution process promptly. The mixture was then centrifuged at 6000 rpm for 10 min to separate DES as supernatants for recycling purpose. The sediments containing CNF were subjected to dialysis using a dialysis membrane (12,000–14,000 Da) against water until a constant pH was attained. Given that not all samples were characterized in solid form, the resultant CNF suspension was not promptly separated from the solution after ultrasonication. The obtained CNF suspension was stored in a refrigerator before characterization.

2.4. Characterization of CNF

2.4.1. Gravimetric yield

The CNF suspension was oven dried at 80 °C to obtain its weight (m_1), and the yield was determined with reference to the weight of raw durian husk fibers (RDHF) using the Eq. (1).

$$\text{Yield} = \frac{m_1}{m_0} \times 100\% \quad (1)$$

2.4.2. Chemical compositional analysis

The chemical composition of the RDHF and CNFs was analysed based on TAPPI standard methods. The lignin content in the samples was characterized using TAPPI T222. In this procedure, 300 mg of extractives-free sample was introduced into 3 mL of 72 % sulfuric acid at 30 °C for 1 h. Subsequently, the acid mixture was diluted to 3 %, boiled for 4 h, and allowed to settle in an inclined position overnight. The sediment obtained was considered acid-insoluble lignin, while the filtered supernatant was collected for acid-soluble lignin determination. The collected acid-insoluble lignin was washed with hot water and dried in a vacuum oven for 1 h at 105 ± 3 °C. Simultaneously, the acid-soluble lignin was determined by measuring the solution's absorbance using UV-Vis spectrophotometry at 205 nm (Eq. (2)).

$$\text{Lignin} = \frac{A}{b \times a} \quad (2)$$

Where A refers to absorbance, b represents the light path in cm, and a denotes the absorptivity in $l \text{ g}^{-1} \text{ cm}^{-1}$. The total lignin content was determined by summing the values of insoluble and soluble lignin contents.

The delignification ratio is calculated using equation below (Eq. (3)):

$$\text{Delignification ratio}(\%) = \left(1 - \frac{\text{Totalsolidafterpretreatment}}{\text{Totalsolidbeforepretreatment}} \right) \times 100\% \quad (3)$$

After drying, 250 mg of the extractives-free samples were mixed with 5 mL of deionized water, 2 mL of acetic acid, and 10 mL of 80 % sodium chlorite. The mixture was heated at 90 °C in a water bath for 1 h. Following this, an additional 4 mL of acetic acid and 10 mL of 80 % sodium chlorite were added to the reaction solution for another hour of reaction. Subsequently, the reaction solution was immersed in a 10 °C water bath to terminate the reaction, and the remaining solids were filtered and washed with deionized water. The remaining solids were quantified as holocellulose (a combination of hemicellulose and cellulose), and they were dried at 105 ± 3 °C until a constant weight was achieved.

In the final step, 100 mg of holocellulose was immersed in 8 mL of 17.5 % NaOH for 30 min at room temperature. Following this, 8 mL of deionized water was added to the solution for a 30 min reaction. Subsequently, the solids were filtered and washed with deionized water. The

residue was impregnated with 20 mL of 1.0 M acetic acid for 5 min. Finally, the residue was washed with excess water and dried at 105 °C until a constant weight was achieved. These remaining residues are quantified as alpha-cellulose, and the difference between the holocellulose and cellulose values provides the hemicellulose content of the samples [29,30].

2.4.3. Fourier transform infra-red spectroscopy (FTIR)

The functional groups and chemical structure of the extracted CNF were analysed using a FTIR spectrometer (Spectrum 100, Perkin Elmer Inc., USA) equipped with an attenuated total reflectance (ATR) diamond accessory, by scanning through 600 to 4000 cm^{-1} with a resolution of 40 scans and 4 cm^{-1} [13,31].

2.4.4. *Uv-vis* spectroscopy

The UV – vis absorption spectrum of 0.5 wt% CNF suspension was obtained at room temperature using an ultraviolet–visible spectrophotometer (JASCO V-770, Jasco Inc., Japan) in the wavelength of 200 to 800 nm.

2.4.5. Morphology analysis

The surface morphology of the obtained CNF was examined using field-emission scanning electron microscopy (FESEM, SU8010, Hitachi Asia Ltd., Japan). CNF suspension was diluted by 100-fold and deposited on a silicon wafer. Subsequently, the samples were sputter-coated with 3 nm of platinum before FESEM observation at an accelerating voltage of 5.0 kV. The average diameter of CNF was measured using Image J software and analysed using Origin software.

3. Results and discussion

In this study, two routes of ultrasound-assisted one-pot CNF synthesis processes, encompassing three sequential steps, i.e., pretreatment of biomass material, isolation of CNF, and surface modification, were conducted using a horn-type ultrasound reactor. The chosen medium for the one-pot CNF synthesis system was a carboxylic acid-based DES, specifically ChCl/OA. The polarity of DES can be enhanced by increasing the presence of hydroxyl and carboxyl groups within the DES. The high polarity of DES is advantageous for establishing hydrogen bonding and solvent interaction between the DES and the lignocellulosic biomass. This improvement facilitates enhanced lignin removal and CNF extraction performance [32–34]. A schematic representation of the experimental process is shown in Fig. 1. An observable transformation occurs in the solvent system, shifting from a transparent state to a wine-red colour upon substituting the RDHF. Furthermore, the solvent system progressively darkens, successfully eliminating lignin and xylan content from the RDHF [35–37]. The process conditions of the as-synthesized CNFs from both protocols were summarized in Table 1. While ultrasonication can enhance the CNF extraction process through defibrillation, it cannot be solely relied upon for the isolation of CNF. Achieving complete extraction requires a chemical or enzymatic pretreatment. While DES can partially disrupt fiber structure, it is not capable of fully isolating CNF. Regrettably, neither ultrasound nor DES alone yielded CNF in the proposed experimental setup. Therefore, data pertaining to ultrasound and DES will be excluded from this study. See Tables 2 and 3.

3.1. Effect of ultrasound irradiation duration on CNF morphologies

The structural and morphological characteristics illustrated in Fig. 2 confirmed the successful yield of nano-sized fibrous cellulose through the post ultrasound treatment and the *in situ* ultrasound-assisted protocol. Fig. 2 (a) and 4(b) depict the surface morphology of CNF samples produced through the post-ultrasound treatment. At the same time, the remaining micrograph illustrates CNF samples synthesized via the proposed *in situ* ultrasound-assisted protocol with varying ultrasound irradiation durations. The fiber width of the produced CNF was randomly

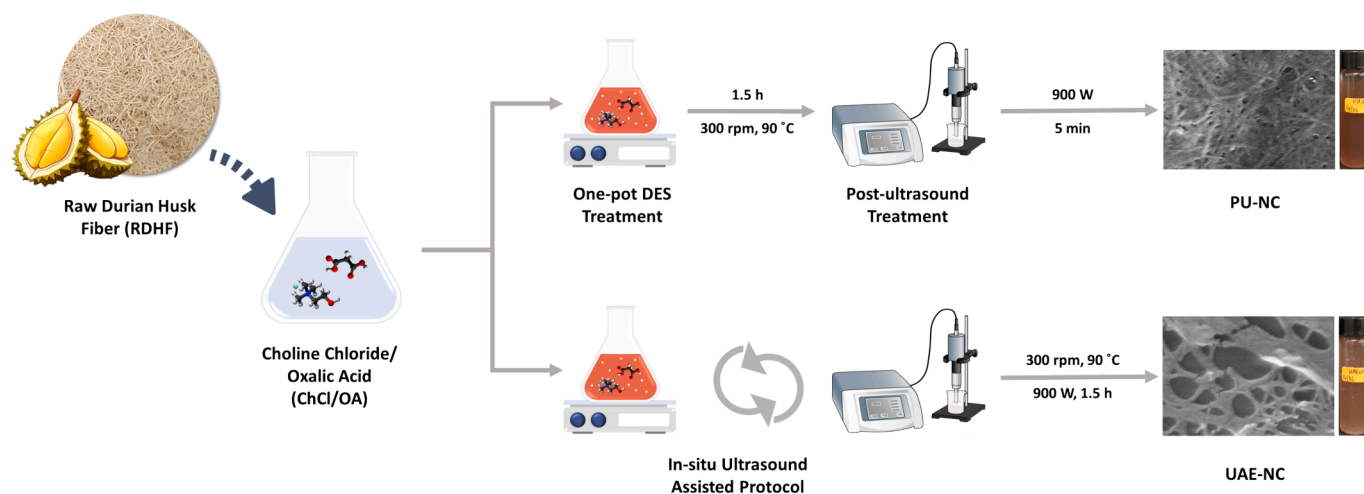


Fig. 1. Schematic illustration of durian husk fiber-derived CNF extraction via one-pot DES treatment with post-ultrasonication treatment and *in situ* ultrasonication treatment.

Table 1
Ultrasound process condition for various sample.

	Process conditions		
	Sonication condition	Irradiation time	Time interval
PU-NC	Post ultrasound treatment	5 min	N/A
UAE 1-NC	<i>in situ</i> ultrasound assisted protocol	1 min	5 min
UAE 2-NC	<i>in situ</i> ultrasound assisted protocol	1 min	7.5 min
UAE 3-NC	<i>in situ</i> ultrasound assisted protocol	1 min	10 min

Table 2
Summary of FTIR Spectra and respective indication.

Wavenumber (cm ⁻¹)	Indication
898	β -glycosidic bond vibration
982	Bending of C-OH and C-H ₃ in hemicellulose
1052	Stretching of C-O bond in cellulose
1161	C-O-C bond stretching vibration
1250	Vibration of C-O stretching in lignin
1316	C-H ₂ wagging in cellulose
1429	Deformation of asymmetric C-H ₂ bond in hemicellulose
1500	Lignin aromatic skeletal vibrations
1730	Vibration of C = O bond of the carboxyl groups in hemicellulose
2890	CH bond stretching vibration
3339	O-H bond stretching vibration

estimated from 50 web-like structural fibres shown in the FESEM micrographs (Fig. 2), and the mean fiber width ranged from 18 to 26 nm. Overall, a web-like heterogeneous interconnected structure was observed on the top surface of all the as-synthesized CNF samples,

Table 3
Compositional analysis of the RDHF and resulting CNFs.

	Lignocellulose composition			Removal content	
	Lignin (%)	Hemicellulose (%)	Cellulose (%)	Lignin (%)	Hemicellulose (%)
Raw durian husk fiber	19.57	40.43	40.00	–	–
PU-NC	11.55	16.03	72.41	40.97	60.35
UAE 1-NC	17.80	7.24	74.96	9.04	82.09
UAE 2-NC	0.11	24.31	75.58	99.44	39.87
UAE 3-NC	0.10	38.36	61.54	99.50	5.12

indicating the successful removal of amorphous cellulose with a random orientation. Indeed, these web-like structures were formed due to the disproportional cleavage of inter- and intra- hydrogen bond networks caused by ultrasound cavitation and the protons released by DES [38,39]. The reduction in fiber size can be attributed to the increased frequency of ultrasound cavitation and protons attacks on the CNF surface. The non-crystalline regions were rapidly and disproportionately destroyed, leading to a substantial increase in pores on the CNF surface and, consequently, a smaller fiber size.

The intense turbulence generated by ultrasound cavitation is crucial in facilitating efficient mixing within the solvent system, effectively reducing diffusion barriers throughout the interconnected structure of durian husk fibres. With the extension of ultrasound irradiation time, the cavitation bubbles generated by ultrasound contribute to the erosion of the biomass structure. Consequently, as liquid movement intensifies and erosion on the biomass structure is enhanced, protons are available within the one-pot system. This increased availability promotes a more frequent attack of protons on the hydrogen bond network within the biomass structure [40]. Consequently, as the ultrasound irradiation time increases, more pores are generated on the cellulose surface, leading to enhanced uniformity in CNF surface pores and facilitating the formation of a web-like structure. FESEM micrograph depicts a crystalline structure stacked on the entangled web-like structure, which suggests the presence of remaining or repolymerized lignin.

3.2. Effect of ultrasound irradiation duration on chemical composition

The identification of lignin in the diluted CNF suspension was accomplished through UV–Vis spectral analysis. As illustrated in Fig. 3a, absorbance peaks corresponding to the aromatic chromophore of lignin (at 230 nm and 280 nm) were observed in all CNF suspensions (0.5 wt%) [41]. Among all the prepared CNF suspensions, PU-NC and UAE 1-NC suspensions exhibited the highest peak intensity at 280 nm, correlating with the visually observed darker colour. This can be attributed to

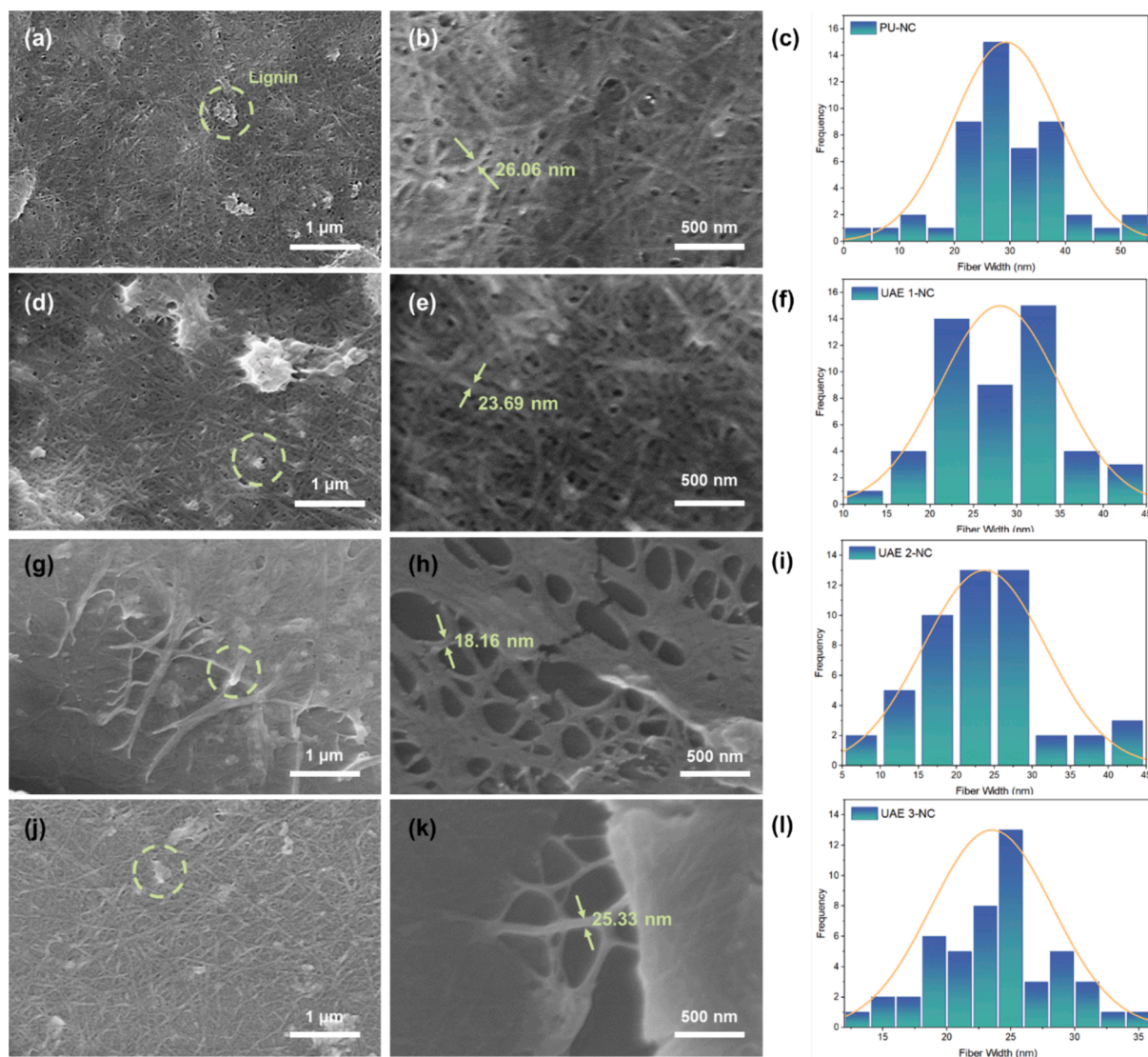


Fig. 2. FESEM micrographs of PU-NC (a) (b), UAE 1-NC (d) (e), UAE 2-NC (g) (h), and UAE 3-NC (j) (k) at 1.0 μm as well as 500 nm; and particle distribution of PU-NC (c), UAE 1-NC (f), UAE 2-NC (i) and UAE 3-NC (l).

the cellulose undergoing a charring process due to the increasingly acidic synthesis environment and residual lignin content. The lignin content within the dissolution system would degrade into an acid-soluble form, further depolymerizing into smaller molecular-weight products. These smaller products would then repolymerize into insoluble lignin residuals deposited on the CNF, contributing to the darkening of the samples. In the case of CNF suspension prepared using the *in situ* ultrasound-assisted protocol, the peak intensity increased as the ultrasound irradiation was reduced. A decrease in ultrasound irradiation interval led to an increase in the frequency of *in situ* ultrasonication, thereby significantly enhancing the DES hydrolysis process. Prolonged hydrolysis processes aided by ultrasound cavitation enhance the extraction of CNF and promote the degradation of lignin content into an acid-soluble form. Additionally, the process leads to the repolymerization of numerous smaller molecular weight products into insoluble lignin residuals. Consequently, the colour of the CNF suspension deepens as the ultrasound irradiation interval decreases, resulting in a higher absorbance requirement at the wavelength of 280 nm. The anomalous peak and high lignin content observed in UAE 1-NC validate the efficacy of *in situ* ultrasonication treatment in catalysing both the biomass disruption process and the repolymerization of high lignin content, attributable to the prolonged process duration [33,35,42].

While all resulting CNF suspensions exhibited strong transmittance at 400 nm, an increment in transmittance was noted across the visible wavelength range (Fig. 3b). Following Rayleigh scattering principles, a direct relationship exists between particle diameter and increased light scattering. Notably, the transmittance values of 0.01 wt% CNF at 600 nm were notably low, measuring at 14.09 %, 22 %, 19.86 %, and 30.63 % for PU-NC, UAE 1-NC, UAE 2-NC, and UAE 3-NC, respectively. The decrease in visible light transmission can be primarily attributed to variations in nanofibril quantities and qualities, including dimensions, surface chemistries, and charges. These relatively lower transmittance values, significantly below those reported in previous studies [18], highlight a complex and entangled structure in the synthesized CNF, leading to minimal visible light scattering. Consequently, the observed lower light scattering in the as-synthesized CNF suspension in this study can be attributed to its intricate and web-like entangled structure [43]. The analysis of lignin distribution in the resulting CNF suspensions was conducted at a fixed wavelength absorption (Fig. 3c). The linear increase in the intensity of the absorbance peak at 280 nm with the rise in CNF suspension, especially in terms of lignin concentration, indicates a homogeneous distribution of lignin within the CNF suspension.

FTIR analysis provides insights into the chemical transformation occurring from RDHF to CNF as a result of DES treatment and various

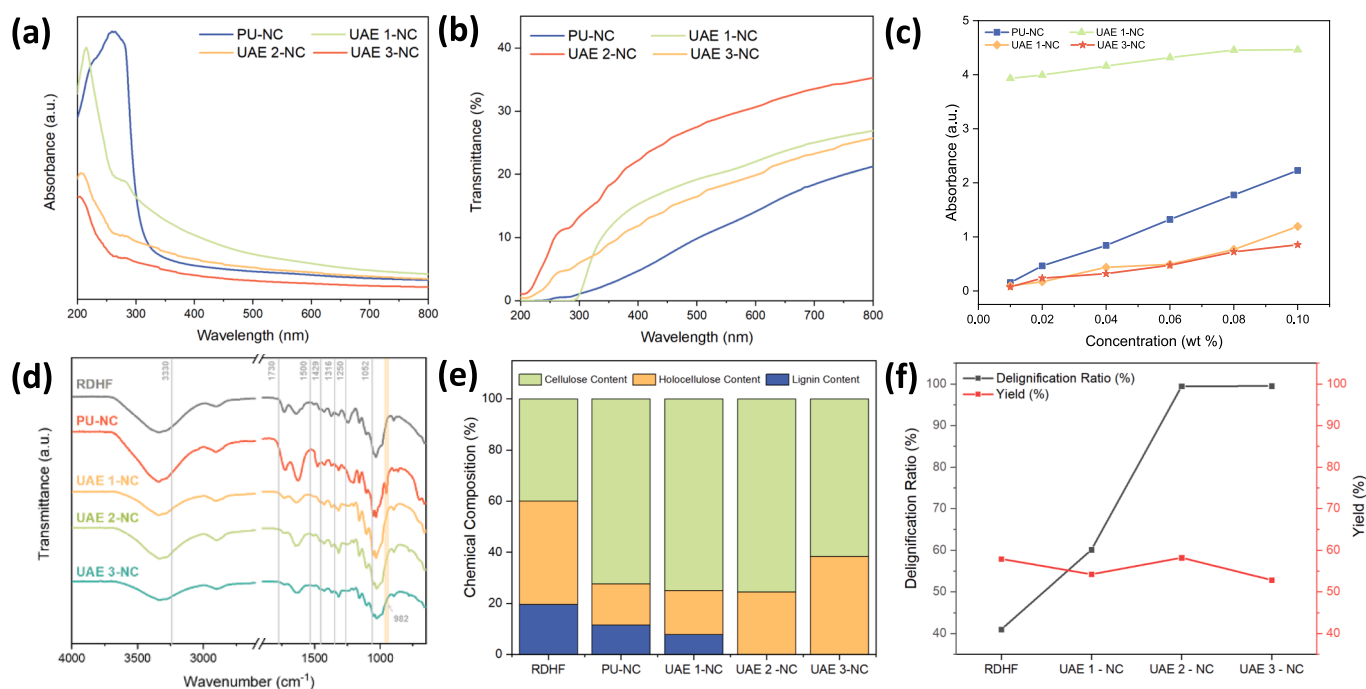


Fig. 3. UV-vis absorbance (a) and transmittance (b) of 0.5 wt% as-synthesized CNF, absorbance at 280 nm vs CNF concentration (c), delignification ratio and CNF yield of as-synthesized CNF (d) fourier transform infrared spectra of RDHF and as-synthesized CNF (e), and chemical composition and solid recovery for as-synthesized CNF (f).

ultrasonication approaches and conditions (Fig. 3d). The cellulose is characterized by the peaks at 3339, 2890, 1429, 1316, 1161, 1052, 898 cm⁻¹, corresponding to the vibrational modes of OH stretching, CH stretching, CH₂ scissoring, CH₂ rocking vibration, C-O-C stretching, C-O stretching, and β-glycosidic bond vibration, respectively [44,45]. These peaks mirror the cellulose I β-assigned peaks found in pristine RDHF, indicating that both DES and ultrasonication processes do not cause alterations in the cellulose polymorphic structure. In contrast to RDHF, all CNF exhibit a significant increase in signal intensity at the water absorption peak of 1644 cm⁻¹, attributing to their characteristic traits of larger specific surface area and hydrophilic nature [46,47]. The functional groups associated with lignin in RDHF, including the vibration of the aromatic in-plane C-O bond and the guaiacyl ring located at 1250 cm⁻¹ and 1500 cm⁻¹ reduced in band intensity after both post-ultrasound and *in situ* ultrasound treatments (Fig. 3d). Particularly, the band at 1250 cm⁻¹ diminished completely after *in situ* treatment, suggesting its more effective lignin dissolution than post-ultrasound treatment. Besides, characteristic peaks of hemicellulose comprise the bending vibration of the C-H₃ and C-OH bonds, the deformation of the asymmetric C-H₂ bond, as well as the stretching of C=O, observed at 982, 1429, and 1730 cm⁻¹, respectively [44,45]. Even following the DES extraction process with post-ultrasound and *in situ* ultrasound treatments, these peaks distinctive of hemicellulose persist, indicating their significant presence in the resulting CNFs. The established standard protocols outlined by TAPPI were implemented to determine the quantitative alterations in composition and assess the corresponding efficiency of pretreatment.

Fig. 3e and Table 4 present the chemical composition of the RDHF and CNF analysed through TAPPI methodology. The RDHF composition comprises 19.57 % lignin, 40.43 % hemicellulose, and 40.00 % cellulose. Treatment with DES followed by post-ultrasonication led to partial dissolution of both hemicellulose and lignin, resulting in removal percentages of 60.35 % and 40.97 %, respectively. Conversely, despite the facilitation of solvent penetration and chemical reactivity by *in situ* sonication in UAE-1, the resultant CNF exhibited lower lignin removal 9.04 % but higher hemicellulose removal 82.09 %. This discrepancy

Table 4
Properties of CNF from different extraction conditions.

	Process condition (sonication time; interval time; number of sonication cycle)	Delignification Ratio (%)	Yield (%)	Average Fiber Width (nm)
PU-NC	5 min; NA; NA	40.97	57.92	26.06
UAE 1-NC	<i>In situ</i> ultrasonication, 1 min irradiation/5 min interval; 1 min; 5 min; 15	9.04	54.22	23.69
UAE 2-NC	<i>In situ</i> ultrasonication, 1 min irradiation/7.5 min interval; 11	99.44	58.22	18.16
UAE 3-NC	<i>In situ</i> ultrasonication, 1 min irradiation/10 min interval; 8	99.50	52.84	25.33

may be attributed to the triggering of lignin repolymerization by the sonication conditions applied in UAE-1. While the cleavage of β-O-4' linkages is pivotal for lignin removal, DES extraction can dissolve substantial pseudo-lignin containing highly-reactive functionalities, inducing the repolymerization of polysaccharide degradation products and consequently reducing the delignification ratio [48]. Studies have previously noted the concurrent occurrence of lignin repolymerization and depolymerization during DES extraction, particularly under harsh conditions, resulting in decreased lignin content in treated fibers compared to optimal conditions [49,50]. See Table 5.

Employing less intensive sonication with longer time intervals and fewer cycles in UAE-2 and UAE-3 treatments significantly improves delignification efficiency, reaching up to 99.44 % and 99.50 %, respectively. The variation in lignin content in CNF prepared under different sonication conditions, as measured using the TAPPI methodology, correlates with aforementioned UV-Vis spectroscopy findings. They particularly both suggest that UAE-2 and UAE-3 provide more favorable sonication conditions, resulting in high delignification ratios beyond 99 %. This significant delignification efficiency achieved

Table 5
Comparison table of the production yield and CNF characteristics.

DES (HBA/HBD)	Molar Ratio	Biomass	Yield (%)	CNF characteristics	Delignification Ratio (%)	Extraction Method	Post treatment method	Ultrasound conditions (frequency nominal power and type)	Ref.
ChCl/OA/water	2:2:1	Coffee Parchment	78.50	Nanofibrils with 10 nm width	38.8	MW-DES/TEMPO-mediated oxidation	Ultrasonication	25 kHz, 190 W, horn	[60]
ChCl/OA	1:3	Raw cotton fiber	81.6	Nanofibrils with 4.69 nm width and 122.4 nm length	–	DES	High power ultrasonic homogenization	20 kHz, 300 W, horn	[61]
ChCl/OA/ AlCl ₃ ●H ₂ O	1:1:0.2	Sugarcane bagasse	62.6	Nanofibrils with 17 nm width and 600 nm length	83.3	MW-DES	Ultrasonication	20 kHz, 650 W, horn	[62]
ChCl/OA	1:1	Luffa sponge	59.1	Nanofibrils with 20 nm width and 2000 nm length	59.4	DES	Ultrasonication	20 kHz, 600 W, horn	[28]
ChCl/OA	1:1	Durian husk fiber	57.92	Web-like nanostructure, 26.06 nm pore size	40.97	DES	Ultrasonication	50 kHz, 900 W, horn	This work
ChCl/OA	1:1	Durian husk fiber	58.22	Web-like nanostructure, 18.16 nm pore size	99.44	<i>In situ</i> ultrasound-assisted one-pot DES treatment		50 kHz, 900 W, horn	This work

through DES combined with *in situ* ultrasound treatment surpasses that of a previous study utilizing ChCl/OA alone without mechanical assistance [51]. Even after optimization from temperatures ranging between 90 to 140 °C, the results of the previous study remained below 80 %. This underscores the enhancing effect of ultrasonication on performance, particularly with *in situ* ultrasound treatment generally yields higher delignification efficiency compared to post-ultrasound treatment, within an optimal range that avoids triggering opposing repolymerization mechanisms. *In situ* ultrasound treatment benefits from *in situ* cavitation, disrupting and exposing biomass structure, enabling deeper penetration of protons from DESs for enhanced reactivity [52,53].

The utilization of DES in conjunction with post-ultrasound treatment and *in situ* ultrasound treatments both facilitated the removal of hemicellulose and lignin, leading to an increased cellulose content compared to RDHF. Despite variations in the efficiency of non-cellulosic removal, both sonication approaches and the various sonication conditions yield similar gravimetric amounts of CNF, ranging from 52.84 % to 58.22 %. This consistency in yield is attributed to the trade-off between enhanced delignification efficiency and reduced hemicellulose removal, which can be attributed to the limited capacity of DES to dissolve non-cellulosic components overall. Similar findings were reported by Hong's group when employing DES combined with post-ultrasound treatment [28]. Nonetheless, nearly complete cellulose retention was consistently observed across all CNF samples, underscoring the suitability of ChCl/OA as a preferred choice for a one-pot system encompassing pretreatment, CNF isolation, and simultaneous surface functionalization. Additionally, the results emphasized the effectiveness of UAE-2, utilizing a 7.5-minute interval for *in situ* ultrasonication irradiation, which optimized CNF yield at 58.22 % with a remarkable 99.44 % delignification ratio. (Fig. 3f).

3.3. Effect of ultrasound treatment on CNF preparation

Carboxylic acid-based DES ChCl/OA has proven effective in breaking down the biomass structure, and the incorporation of ultrasound irradiation significantly enhances the penetration of protons and hydrolysis efficiency. Table 4 summarizes the properties of CNF produced under different extraction conditions, including delignification ratio, yield, and the average width of the fiber. Taking a comprehensive perspective, the suggested ultrasound-assisted one-pot DES treatment consistently yields CNF ranging from 52 % to 58 %, with fiber widths falling within the range of 18 nm to 26 nm. When examining the residual lignin content in the synthesized CNF, post-ultrasonication treatment leads to CNF with a lower delignification ratio. In contrast, employing *in situ* ultrasonication treatment with optimal irradiation intervals results in CNF exhibiting an elevated delignification ratio, highlighting the

effectiveness of biomass pretreatment during the *in situ* ultrasound-assisted protocol.

Table 4 provides a comparative analysis of the CNF yield and characteristics obtained in our study with those from prior research endeavors, wherein DESs and ultrasound treatment served as the principal extraction and post-treatment methodologies, respectively. The CNF yield from post-ultrasound and *in situ* ultrasound-assisted protocol aligns with findings from earlier studies. Notably, the CNF yield derived from both the post-ultrasound and *in situ* ultrasound-assisted protocols is not significantly different from earlier studies. Instead, it was noted that this study shows a higher delignification ratio but a slightly lower yield compared to previous literatures. This diminished yield can be attributed to several factors, including the absence of water addition and microwave assistance (MW), as well as the DES molar ratio used in this study. Whilst, the superior delignification ratio obtained through *in situ* ultrasound-assisted protocol suggests that this treatment prioritized biomass pretreatment over CNF isolation. Interestingly, it is quintessential to highlight that the surface morphology of the as-produced CNF in this study differs from that in prior work. Instead of the typical nanorod or nanofibril structure, a web-like structure was observed in the CNF produced here. This unique web-like structure can be ascribed to the disproportionate attack of free anions on the cellulose surface, deviating from the unidirectional hydrogen bond cleavage that typically shortens CNF sizes. Recent studies have focused on transforming conventional rod-like CNF into a web-like structure to enhance accessibility and mechanical strength in various applications, such as membrane separation and energy conversion [54–57]. Earlier research efforts involved time-consuming and resource-intensive methods like templating, freeze-drying, and TEMPO-oxidation for CNF production [58,59]. Therefore, this study's facile one-pot synthesis process allows for the direct and greener production of web-like CNF, offering a more feasible approach.

Throughout the process, ultrasonication plays distinct roles across various phases of the one-pot DES treatment. Fig. 4 summarized and compared the disruption pathway of the biomass interconnected network through both the post-ultrasound treatment and the *in situ* ultrasound-assisted protocol. Post-ultrasonication, when integrated, effectively reduces the size of the extracted CNF. In this process route, cellulose is initially extracted through the one-pot DES treatment, followed by a sequential cell disruption process facilitated by post-ultrasonication treatment. Simultaneously, *in situ* ultrasonication plays a crucial role in enhancing the accessibility of the solvent and catalysing the reaction [63,64]. During the *in situ* ultrasound-assisted protocol, the ultrasonication irradiation generates the implosion of cavitation microbubbles. These cavitation bubbles significantly enhance the movement of reactants among the reaction sites, thereby improving mass and heat transfer within the reaction medium, and disrupt the

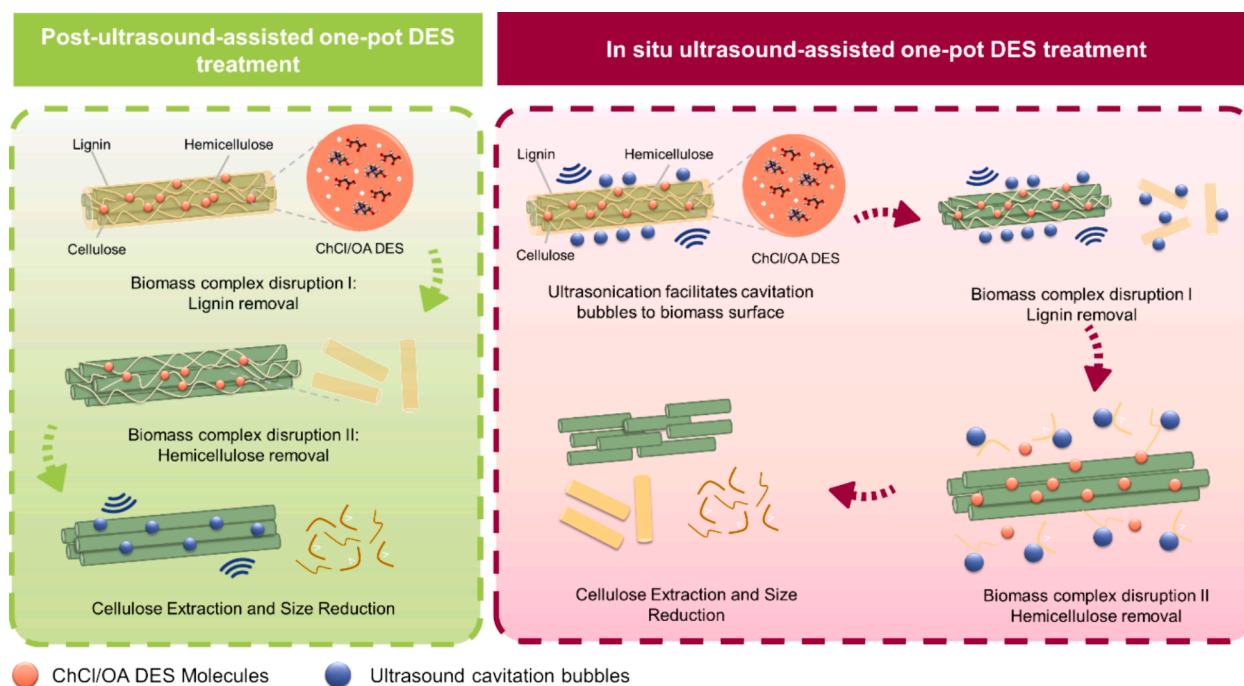


Fig. 4. Schematic diagram of the biomass structure breakdown process through ultrasound-assisted one-pot DES treatment.

robust durian husk fiber structure effectively. Consequently, this enhances the penetration of DES into the entangled biomass matrix, increasing the interfacial contact between the DES and the entangled biomass matrix [65]. By increasing biomass exposure, the enhanced availability of protons released by the DES facilitates effective proton attacks on the hydrogen bond network within the biomass structure [66]. The proton-abundant ChCl/OA, characterised by high carboxyl and hydroxyl groups, exhibits notable efficiency in lignin removal and yields significant amount of CNF. These synergistic effects of both post and *in situ* ultrasonication treatments manifest in the lower lignin content observed in the latter treatment.

4. Conclusion

This study introduces a novel and environmentally friendly approach to one-pot CNF preparation, successfully synthesizing CNF with concurrent and consecutive ultrasonication in a horn-type ultrasonic reactor. Integrating this benign *in situ* ultrasonication-assisted one-pot extraction method with a 7.5 min interval yields a relatively high CNF output of 58.22 %, with nearly zero lignin content (0.1 %). The study findings indicate that *in situ* ultrasonication enhances the penetration of DES through the durian husk fiber biomass structure and significantly increases the disruption of hydrogen bonds. By varying the ultrasound irradiation time, the CNF with web-like structures reveals that lower lignin content can be successfully obtained. CNF synthesized through *in situ* ultrasound-assisted one-pot extraction holds promise for various applications, including environmental remediation, membrane separation, and drug delivery.

CRediT authorship contribution statement

Jocelyn Jean Yi Lim: Writing – review & editing, Writing – original draft, Methodology, Investigation, Formal analysis, Conceptualization. **Do Yee Hoo:** Writing – review & editing, Writing – original draft, Methodology, Formal analysis, Conceptualization. **Siah Ying Tang:** Writing – review & editing, Resources. **Sivakumar Manickam:** Writing – review & editing. **Lih Jiun Yu:** Writing – review & editing, Conceptualization. **Khang Wei Tan:** Writing – review & editing, Validation,

Supervision, Funding acquisition, Conceptualization.

Declaration of competing interest

The authors declare that they have no known competing financial interests or personal relationships that could have appeared to influence the work reported in this paper.

Acknowledgements

The authors would like to acknowledge the financial support from Durian Garden Sdn. Bhd. (EENG/0012) and Xiamen University Malaysia through the Xiamen University Malaysia Research Fund (XMUMRF/2022-C10/IENG/0048).

References

- [1] R. Nunta, C. Techapun, S. Sommanee, C. Mahakuntha, K. Porninta, W. Punyodom, Y. Phimolsiripol, P. Rachtanapun, W. Wang, X. Zhuang, W. Qi, K. Jantanasakulwong, A. Reungsang, A. Kumar, N. Leksawasdi, Valorization of rice straw, sugarcane bagasse and sweet sorghum bagasse for the production of bioethanol and phenylacetylcarbinol, *Sci. Rep.* 13 (2023) 727.
- [2] A. Selvarajoo, C.W. Lee, D. Oochit, K.H.O. Almashjary, Bio-pellets from empty fruit bunch and durian rinds with cornstarch adhesive for potential renewable energy, *Mater. Sci. Energy Technol.* 4 (2021) 242–248.
- [3] M.A. Siti Nur E'zzati, H. Anuar, A.R. Siti Munirah Salimah, Effect of coupling agent on durian skin fibre nanocomposite reinforced polypropylene, *IOP Conf. Series: Mater. Sci. Eng.* 290 (2018) 012032.
- [4] J. Gao, Y. Qiu, F. Chen, L. Zhang, W. Wei, X. An, Q. Zhu, Pomelo peel derived nanocellulose as Pickering stabilizers: Fabrication of Pickering emulsions and their potential as sustained-release delivery systems for lycopene, *Food Chem.* 415 (2023) 135742.
- [5] A. Tshikovhi, S.B. Mishra, A.K. Mishra, Nanocellulose-based composites for the removal of contaminants from wastewater, *Int. J. Biol. Macromol.* 152 (2020) 616–632.
- [6] S.S. Ahankari, A.R. Subhedar, S.S. Bhadauria, A. Dufresne, Nanocellulose in food packaging: a review, *Carbohydr. Polym.* 255 (2021) 117479.
- [7] T. Xu, H. Du, H. Liu, W. Liu, X. Zhang, C. Si, P. Liu, K. Zhang, Advanced nanocellulose-based composites for flexible functional energy storage devices, *Adv. Mater.* 33 (2021) 2101368.
- [8] A. Saddique, I.W. Cheong, Recent advances in three-dimensional bioprinted nanocellulose-based hydrogel scaffolds for biomedical applications, *Korean J. Chem. Eng.* 38 (2021) 2171–2194.

- [9] H. Ibrahim, N. Sazali, W.N.W. Salleh, A.F. Ismail, Nanocellulose-based materials and recent application for heavy metal removal, *Water Air Soil Pollut.* 232 (2021) 305.
- [10] M. Thakur, A. Sharma, V. Ahlawat, M. Bhattacharya, S. Goswami, Process optimization for the production of cellulose nanocrystals from rice straw derived α -cellulose, *Mater. Sci. Energy Technol.* 3 (2020) 328–334.
- [11] Y. Xie, J. Zhao, P. Wang, Z. Ling, Q. Yong, Natural arginine-based deep eutectic solvents for rapid microwave-assisted pretreatment on crystalline bamboo cellulose with boosting enzymatic conversion performance, *Bioresour. Technol.* 385 (2023) 129438.
- [12] Q. Liu, T. Yuan, Q.-J. Fu, Y.-Y. Bai, F. Peng, C.-L. Yao, Choline chloride-lactic acid deep eutectic solvent for delignification and nanocellulose production of moso bamboo, *Cellul.* 26 (2019) 9447–9462.
- [13] W.-L. Lim, A.A.N. Gunny, F.H. Kasim, S.C.B. Gopinath, N.H.I. Kamaludin, D. Arbain, Cellulose nanocrystals from bleached rice straw pulp: acidic deep eutectic solvent versus sulphuric acid hydrolyses, *Cellul.* 28 (2021) 6183–6199.
- [14] W. Yu, C. Wang, Y. Yi, H. Wang, Y. Yang, L. Zeng, Z. Tan, Direct pretreatment of raw ramie fibers using an acidic deep eutectic solvent to produce cellulose nanofibrils in high purity, *Cellul.* 28 (2021) 175–188.
- [15] P. Li, Y. Wang, Q. Hou, H. Liu, H. Lei, B. Jian, X. Li, Preparation of cellulose nanofibrils from okara by high pressure homogenization method using deep eutectic solvents, *Cellul.* 27 (2020) 2511–2520.
- [16] N. Huda Syazwani Jafri, D. Noraini Jimat, W. Mohd Fazli Wan Nawawi, Y. Ahmad Nor, A. Amid, Screening of deep eutectic solvent mixtures for treating empty fruit bunches to obtain cellulose nanofiber, *Mater. Today: Proc.* (2023).
- [17] Y. Xu, S.-C. Sun, C. Zhang, C.-Y. Ma, J.-L. Wen, T.-Q. Yuan, Complete valorization of bamboo biomass into multifunctional nanomaterials by reactive deep eutectic solvent pretreatment: Towards a waste-free biorefinery, *Chem. Eng. J.* 462 (2023) 142213.
- [18] J. Jiang, N.C. Carrillo-Enrriquez, H. Oguzlu, X. Han, R. Bi, J.N. Saddler, R.-C. Sun, F. Jiang, Acidic deep eutectic solvent assisted isolation of lignin containing nanocellulose from thermomechanical pulp, *Carbohydr. Polym.* 247 (2020) 116727.
- [19] C.-Y. Ma, X. Gao, X.-P. Peng, Y.-F. Gao, J. Liu, J.-L. Wen, T.-Q. Yuan, Microwave-assisted deep eutectic solvents (DES) pretreatment of control and transgenic poplars for boosting the lignin valorization and cellulose bioconversion, *Ind. Crop. Prod.* 164 (2021) 113415.
- [20] Z. Ling, W. Tang, Y. Su, L. Shao, P. Wang, Y. Ren, C. Huang, C. Lai, Q. Yong, Promoting enzymatic hydrolysis of aggregated bamboo crystalline cellulose by fast microwave-assisted dicarboxylic acid deep eutectic solvents pretreatments, *Bioresour. Technol.* 333 (2021) 125122.
- [21] J. Li, Z. Chen, H. Shi, J. Yu, G. Huang, H. Huang, Ultrasound-assisted extraction and properties of polysaccharide from Ginkgo biloba leaves, *Ultrason. Sonochem.* 93 (2023) 106295.
- [22] K. Kumar, S. Srivastav, V.S. Sharanagat, Ultrasound assisted extraction (UAE) of bioactive compounds from fruit and vegetable processing by-products: A review, *Ultrason. Sonochem.* 70 (2021) 105325.
- [23] N. Sanwal, S. Mishra, J.K. Sahu, S.N. Naik, Effect of ultrasound-assisted extraction on efficiency, antioxidant activity, and physicochemical properties of sea buckthorn (*Hippophae salicifolia*) seed oil, *LWT* 153 (2022) 112386.
- [24] D.Y. Hoo, Z.L. Low, D.Y.S. Low, S.Y. Tang, S. Manickam, K.W. Tan, Z.H. Ban, Ultrasonic cavitation: An effective cleaner and greener intensification technology in the extraction and surface modification of nanocellulose, *Ultrason. Sonochem.* 90 (2022) 106176.
- [25] J. Guo, X. Guo, S. Wang, Y. Yin, Effects of ultrasonic treatment during acid hydrolysis on the yield, particle size and structure of cellulose nanocrystals, *Carbohydr. Polym.* 135 (2016) 248–255.
- [26] K.T.T. Amesho, Y.-C. Lin, S.V. Mohan, S. Halder, V.K. Ponnusamy, S.-R. Jhang, Deep eutectic solvents in the transformation of biomass into biofuels and fine chemicals: a review, *Environ. Chem. Lett.* (2022).
- [27] Y. Bai, X.-F. Zhang, Z. Wang, T. Zheng, J. Yao, Deep eutectic solvent with bifunctional Brønsted-Lewis acids for highly efficient lignocellulose fractionation, *Bioresour. Technol.* 347 (2022) 126723.
- [28] S. Hong, Y. Song, Y. Yuan, H. Lian, H. Liimatainen, Production and characterization of lignin containing nanocellulose from luffa through an acidic deep eutectic solvent treatment and systematic fractionation, *Ind. Crop. Prod.* 143 (2020) 111913.
- [29] S. Triyani, S. Herman, Harmita, Sutriyo, Comparison of the deep eutectic solvent (DES) solvent for extracting lignin from the lignocellulosic material of pineapple leaves, *Pharmacognosy J.* 13 (2021).
- [30] C.M. Pacheco, C. Bustos, G. Reyes, M.G. Aguayo, O.J. Rojas, Characterization of residues from Chilean blueberry bushes: a potential source of cellulose, *BioResources* 13 (2018) 7345–7359.
- [31] L. Douard, J. Bras, T. Encinas, M.N. Belgacem, Natural acidic deep eutectic solvent to obtain cellulose nanocrystals using the design of experience approach, *Carbohydr. Polym.* 252 (2021) 117136.
- [32] Y.T. Tan, G.C. Ngoh, A.S.M. Chua, Effect of functional groups in acid constituent of deep eutectic solvent for extraction of reactive lignin, *Bioresour. Technol.* 281 (2019) 359–366.
- [33] F. Mohd Fuad, M. Mohd Nadzir, A. Harun@Kamaruddin, Hydrophilic natural deep eutectic solvent: a review on physicochemical properties and extractability of bioactive compounds, *J. Mol. Liq.* 339 (2021) 116923.
- [34] H. Palmelund, M.P. Andersson, C.J. Asgreen, B.J. Boyd, J. Rantanen, K. Löbmann, Tailor-made solvents for pharmaceutical use? Experimental and computational approach for determining solubility in deep eutectic solvents (DES), *International Journal of Pharmaceutics: X* 1 (2019) 100034.
- [35] M. Parot, D. Rodrigue, T. Stevanovic, High purity softwood lignin obtained by an eco-friendly organosolv process, *Bioresource Technology Reports* 17 (2022) 100880.
- [36] Y. Zhang, A.N. Haque, M. Naebe, Lignin–Cellulose Nanocrystals from Hemp Hurd as Light-Coloured Ultraviolet (UV) Functional Filler for Enhanced Performance of Polyvinyl Alcohol Nanocomposite Films, in, *Nanomaterials* (2021).
- [37] Q. Zhai, S. Han, C.-Y. Hse, J. Jiang, J. Xu, 5-Sulfosalicylic acid as an acid hydrotrope for the rapid and green fractionation of woody biomass, *Ind. Crop. Prod.* 177 (2022) 114435.
- [38] Y. Xie, J. Zhao, P. Wang, Z. Ji, Z. Ling, Q. Yong, Microwave-assisted fast co-production of fermentable sugar and nanocellulose via tunable zinc acetate based deep eutectic solvents treatments, *Ind. Crop. Prod.* 191 (2023) 115965.
- [39] V. Midhun, S. Suresh, P. Praveen, R. Neethikumar, K. Rajesh, Preparation, characterisation and thermal property study of micro/nanocellulose crystals for vacuum insulation panel application, *Thermal Sci. Eng. Progress* 25 (2021) 101045.
- [40] E.M.M. Flores, G. Cravotto, C.A. Bizzi, D. Santos, G.D. Iop, Ultrasound-assisted biomass valorization to industrial interesting products: state-of-the-art, perspectives and challenges, *Ultrason. Sonochem.* 72 (2021) 105455.
- [41] J. Jiang, N.C. Carrillo-Enrriquez, H. Oguzlu, X. Han, R. Bi, M. Song, J.N. Saddler, R.-C. Sun, F. Jiang, High production yield and more thermally stable lignin-containing cellulose nanocrystals isolated using a ternary acidic deep eutectic solvent, *ACS Sustain. Chem. Eng.* 8 (2020) 7182–7191.
- [42] T. Suopajarvi, P. Ricci, V. Karvonen, G. Ottolina, H. Liimatainen, Acidic and alkaline deep eutectic solvents in delignification and nanofibrillation of corn stalk, wheat straw, and rapeseed stem residues, *Ind. Crop. Prod.* 145 (2020) 111956.
- [43] G.D. Patterson, W.J. Orts, J.D. McManus, Y.-L. Hsieh, Cellulose and lignocellulose nanofibrils and amphiphilic and wet-resilient aerogels with concurrent sugar extraction from almond hulls, *ACS Agri. Sci. Technol.* 3 (2023) 140–151.
- [44] X. Liu, C.M.G.C. Renard, S. Bureau, C. Le Bourvellec, Revisiting the contribution of ATR-FTIR spectroscopy to characterize plant cell wall polysaccharides, *Carbohydr. Polym.* 262 (2021) 117935.
- [45] K.C. Teh, M.L. Foo, C.W. Ooi, I.M. Leng Chew, Sustainable and cost-effective approach for the synthesis of lignin-containing cellulose nanocrystals from oil palm empty fruit bunch, *Chemosphere* 267 (2021) 129277.
- [46] M. Abdel-Hamied, R.R.A. Hassan, M.Z.M. Salem, T. Ashraf, M. Mohammed, N. Mahmoud, Y.S. El-din, S.H. Ismail, Potential effects of nano-cellulose and nano-silica/polyvinyl alcohol nanocomposites in the strengthening of dyed paper manuscripts with madder: an experimental study, *Sci. Rep.* 12 (2022) 19617.
- [47] R.K. Gond, M.K. Gupta, M. Jawaid, Extraction of nanocellulose from sugarcane bagasse and its characterization for potential applications, *Polym. Compos.* 42 (2021) 5400–5412.
- [48] J. Li, G. Henriksson, G. Gellerstedt, Lignin depolymerization/repolymerization and its critical role for delignification of aspen wood by steam explosion, *Bioresour. Technol.* 98 (2007) 3061–3068.
- [49] Z. Chen, W.A. Jacoby, C. Wan, Ternary deep eutectic solvents for effective biomass deconstruction at high solids and low enzyme loadings, *Bioresour. Technol.* 279 (2019) 281–286.
- [50] S. Wang, H. Li, L.-P. Xiao, G. Song, Unraveling the Structural Transformation of Wood Lignin During Deep Eutectic Solvent Treatment, *Front. Energy Res.* 8 (2020).
- [51] X. Li, W. Tang, Y.-C. He, Integrated understanding of acidic deep eutectic solvent choline chloride: oxalic acid pretreatment to enhance the enzymatic hydrolysis of rape straw, *Ind. Crop. Prod.* 206 (2023) 117691.
- [52] T. El Achkar, S. Fourmentin, H. Greige-Gerges, Deep eutectic solvents: An overview on their interactions with water and biochemical compounds, *J. Mol. Liq.* 288 (2019) 111028.
- [53] X.-D. Hou, K.-P. Lin, A.-L. Li, L.-M. Yang, M.-H. Fu, Effect of constituents molar ratios of deep eutectic solvents on rice straw fractionation efficiency and the micro-mechanism investigation, *Ind. Crop. Prod.* 120 (2018) 322–329.
- [54] S. Ahankari, T. George, A. Subhedar, K.K. Kar, Nanocellulose as a sustainable material for water purification, *SPE Polymers* 1 (2020) 69–80.
- [55] Y. Huang, P. Yang, F. Yang, C. Chang, Self-supported nanoporous lysozyme/nanocellulose membranes for multifunctional wastewater purification, *J. Membr. Sci.* 635 (2021) 119537.
- [56] T. Yeamsuksawat, Y. Morishita, J. Shirahama, Y. Huang, T. Kasuga, M. Nogi, H. Koga, Semicarbonized Subwavelength-Nanopore-Structured Nanocellulose Paper for Applications in Solar Thermal Heating, *Chem. Mater.* 34 (2022) 7379–7388.
- [57] S. Zhou, Z. Qiu, M. Strømme, C. Xu, Solar-driven ionic power generation via a film of nanocellulose @ conductive metal-organic framework, *Energ. Environ. Sci.* 14 (2021) 900–905.
- [58] C. Chen, L. Hu, Nanocellulose toward advanced energy storage devices: structure and electrochemistry, *Acc. Chem. Res.* 51 (2018) 3154–3165.
- [59] K. De France, Z. Zeng, T. Wu, G. Nyström, Functional materials from nanocellulose: utilizing structure-property relationships in bottom-up fabrication, *Adv. Mater.* 33 (2021) 2000657.
- [60] P. Panyamao, S. Charumane, J. Ruangsuriya, C. Saenjum, Efficient Isolation of Cellulosic Fibers from Coffee Parchment via Natural Acidic Deep Eutectic Solvent Pretreatment for Nanocellulose Production, *ACS Sustain. Chem. Eng.* 11 (2023) 13962–13973.
- [61] Z. Ling, J.V. Edwards, Z. Guo, N.T. Prevost, S. Nam, Q. Wu, A.D. French, F. Xu, Structural variations of cotton cellulose nanocrystals from deep eutectic solvent treatment: micro and nano scale, *Cellul.* 26 (2019) 861–876.
- [62] Q. Ji, X. Yu, A.-E.-G.-A. Yagoub, L. Chen, C. Zhou, Efficient cleavage of strong hydrogen bonds in sugarcane bagasse by ternary acidic deep eutectic solvent and

- ultrasonication to facile fabrication of cellulose nanofibers, *Cellul.* 28 (2021) 6159–6182.
- [63] Q. Ji, X. Yu, A.-E.-G.-A. Yagoub, L. Chen, C. Zhou, Efficient removal of lignin from vegetable wastes by ultrasonic and microwave-assisted treatment with ternary deep eutectic solvent, *Ind. Crop. Prod.* 149 (2020) 112357.
- [64] X. Fu, D. Wang, T. Belwal, Y. Xu, L. Li, Z. Luo, Sonication-synergistic natural deep eutectic solvent as a green and efficient approach for extraction of phenolic compounds from peels of *Carya cathayensis* Sarg, *Food Chem.* 355 (2021) 129577.
- [65] F. Verdini, E. Calcio Gaudino, G. Grillo, S. Tabasso, G. Cravotto, Cellulose Recovery from Agri-Food Residues by Effective Cavitation Treatments, in, *Appl. Sci.* (2021).
- [66] A. Ali Redha, Review on extraction of phenolic compounds from natural sources using green deep eutectic solvents, *J. Agric. Food Chem.* 69 (2021) 878–912.